PROCEEDINGS OF SCIENCE

The Music of KOTO: $K_L^0 \to \pi^0 \nu\bar{\nu}$.

Joseph Comfort, for the KOTO Collaboration[*†]
Arizona State University
E-mail: joseph.comfort@asu.edu

The KOTO experiment at the J-PARC laboratory seeks to obtain the first observation of the $K_L^0 \to \pi^0 \nu\bar{\nu}$ decay, as a direct measurement of the CP-violating parameter in the Standard Model. Many improvements are being made over the previous upper limit established by the KEK E391a experiment. The first short-term goal is to get below the Grossman-Nir limit in the first physics run in early 2013.

The XIth International Conference on Heavy Quarks and Leptons
11-15 June, 2012
Prague,The Czech Republic

[*]Speaker.

[†]KEK, Kyoto, NDA, Okayama, Osaka, Saga, Yamagata, ASU, Chicago, Michigan, Cheju, CNU, KNU, PNU, NTU, JINR.

PoS(HQL 2012)017

1. Introduction

The neutral kaons K^0 and $\overline{K^0}$ have had a major role in the development of the Standard Model (SM). In terms of current terminology, associated production (*e.g.*, $\pi^- p \to K^0 \Lambda^0$) opened the door beyond the first-generation u and d quarks to include the s quark. The strong suppression of the decay $K_L^0 \to \mu^+\mu^-$, together with Cabibbo's interpretation of other suppressed decays [1], led to the proposal of a fourth quark to provide a cancellation of amplitudes through the GIM mechanism [2], thereby completing the second generation. The charm c quark was clearly identified four year later.

More pertinent to the topic of this paper was the discovery of CP violation in the decay $K_L^0 \to 2\pi$ compared to the dominant 3π mode [3]. The CKM matrix of Kobayashi and Maskawa [4] accounted for CP violation by introducing a third generation of quarks along with an imaginary quantity (η) needed to preserve unitarity. In combination with non-conservation of baryon number and non-equilibrium conditions in the early universe, CP violation contributes to the very strong observed matter-antimatter asymmetry in the universe.

Kaons provided the only evidence of CP violation for nearly four decades, when such violation was also found in the B system. As discussed elsewhere in this conference, the B system continues to be explored for additional CP-violating processes. The focus is now on the question as to whether physics Beyond the Standard Model (BSM) is needed. The kaon system may yet hold more surprises for us.

2. The $K_L^0 \to \pi^0 \nu\bar{\nu}$ Decay.

The $K_L^0 \to \pi^0 \nu\bar{\nu}$ decay mode provides one of the most direct measures of CP violation. The one-loop diagrams for the $s \to d$ transition are shown in Fig. 1. Because the contributions from the u quark can be expressed via CKM unitarity in terms of the c and t quarks, and because those from the t quark dominate, the decay rate is nearly directly proportional to the CP-violating parameter η^2.

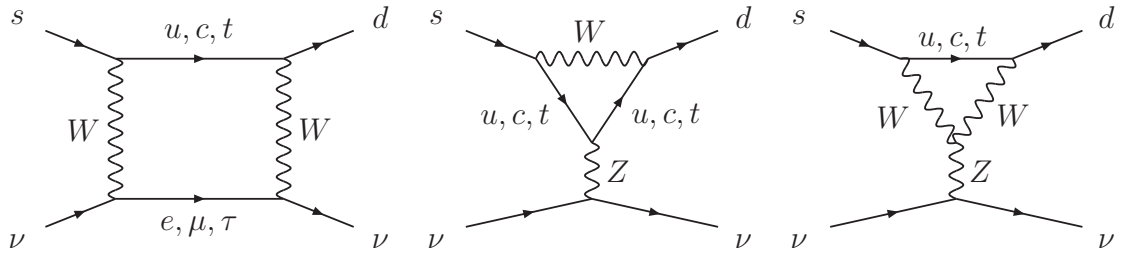

Figure 1: One-loop electroweak diagrams for $K \to \pi\nu\bar{\nu}$ decays.

The predicted SM branching ratios for the $K_L^0 \to \pi^0 \nu\bar{\nu}$ and the analogue $K^+ \to \pi^+ \nu\bar{\nu}$ decay modes are [5]

$$\begin{aligned} K^+ &: (7.81^{+0.72}_{-0.64} \pm 0.43) \times 10^{-11}, \\ K_L^0 &: (2.43^{+0.39}_{-0.36} \pm 0.11) \times 10^{-11}, \end{aligned} \tag{2.1}$$

where the first uncertainty in each case stems from the CKM matrix and the second is a combination of other theory uncertainties. The experimental branching ratios for the two modes are

$$\begin{aligned} &\text{Expt. } \mathscr{B}(K^+ \to \pi^+ \nu\bar{\nu}) = (1.73^{1.15}_{-1.05}) \times 10^{-10} \quad [6], \\ &\text{Expt. } \mathscr{B}(K_L^0 \to \pi^0 \nu\bar{\nu}) \quad < 2.6 \times 10^{-8} \qquad\qquad [7]\,. \end{aligned} \tag{2.2}$$

The upper limit for the K_L^0 mode was recently established at the 90% confidence level in the E391a experiment at the KEK 12-GeV Proton Synchrotron.

From isospin relations, the K^+ decay rate sets an upper limit on the K_L^0 rate: $\mathscr{B}(K_L^0 \to \pi^0 \nu\bar{\nu}) < 4.4 \times \mathscr{B}(K^+ \to \pi^+ \nu\bar{\nu})$ [8]. While the K^+ rate is consistent with the SM within errors, the limit on the K_L^0 rate is a factor of 15–90 above the corresponding Grossman-Nir (GN) limit.

The KOTO[1] experiment, being prepared at the J-PARC Laboratory in Japan, is a successor to the E391a experiment. It is intended to obtain the first observations of the $K_L^0 \to \pi^0 \nu\bar{\nu}$ decay, and ultimately as many as 100 SM events. Its measurement is one of the incisive "golden" experiments in flavor physics today, due to its small theoretical ambiguities in the Standard Model, and also in many extensions of the SM.

Considering the precision with which the K-decay rates can be computed, and their importance for critical SM tests, new experiments dedicated to their measurement are compelling. There are many ideas and models for physics BSM, which need not be discssed here.

A very pertinent example is that provided by Buras *et al.* who made a comprehensive and consistent study of flavor violations in a 4-generation model [9]. They found that the K_L^0 branching ratio can be enhanced by as much as a factor of 40 over the SM. Even more significantly, as shown in Fig. 2, their global analysis yields a solution region just below the Grossman-Nir limit. Similar large values were also found, for example, by Hattori *et al.* [10]. *Hence, New Physics could be lurking just below the GN limit.*

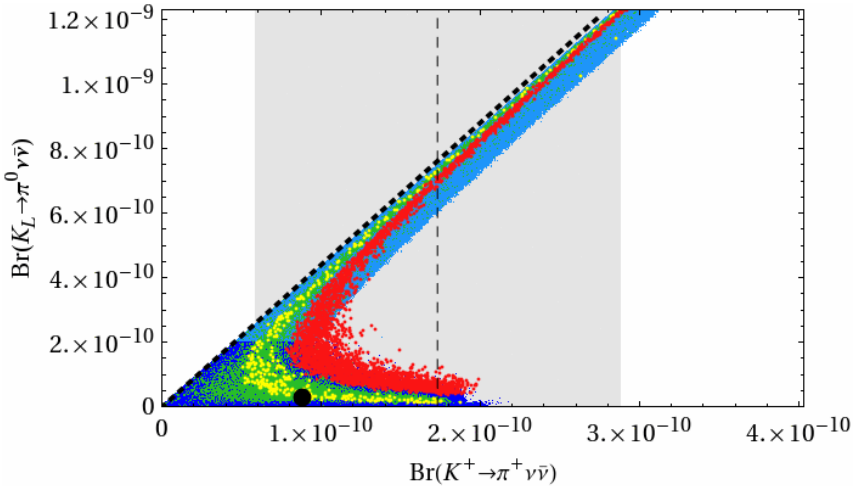

Figure 2: The K_L^0 BR as a function of the K^+ BR. The black point represents the SM value and the shaded region corresponds to the experimental K^+ BR. The dotted line represents the Grossman-Nir limit, and the blue points are the result of the global analysis. The other colors represent variations in some parameters.

[1] $\underline{K^0}$ at $\underline{\text{TO}}$kai. A koto is also a long Japanese stringed instrument played by plucking.

3. The KOTO Experiment

The KOTO experiment is an exceptionally difficult one. The necessary requirements for it and the design of the experiment are well described in the full paper on the E391a experiment [7]. The signal for the $K_L^0 \to \pi^0 \nu \bar{\nu}$ decay is detection of exactly two photons with an invariant mass of a π^0, and nothing else. In short, the goal can be achieved through kinematic constraints, as much of the 4π solid angle as possible, a hermetic detector with high vacuum, thorough knowledge of component detector efficiencies, and identification and suppression by many order of magnitude of all possible backgrounds from the beam and other, much more dominant, decay modes.

The background decay mode of largest concern is $K_L^0 \to \pi^0\pi^0$ with a $\sim$0.1% branching ratio. Other important backgrounds include $K_L^0 \to 3\pi$ (including $3\pi^0$ and $\pi^+\pi^-\pi^0$), $K_L^0 \to \gamma\gamma$, and K_{e3} decays. If not vetoed, charged particles can generate signals that mimic photons or, if present at the same time as a good event, lead to rejection of the signal of interest. Serious backgrounds can also be produced from other particles such as neutrons and photons from the production target. Neutrons in the beam halo that hit collimating materials can also produce π^0s and ηs, which can simulate the signal of interest.

The K_L^0's are produced by a 30-GeV proton beam on a rotating, water-cooled stack of nickel disks. At full intensity, the beam will provide about 2×10^{14} protons per 0.7-s spill, with a repetition rate of 3.3 s. Secondary particles will be extracted at 16° into a beam line that extends 21 meters to the KOTO detector, sketched in Fig. 3.

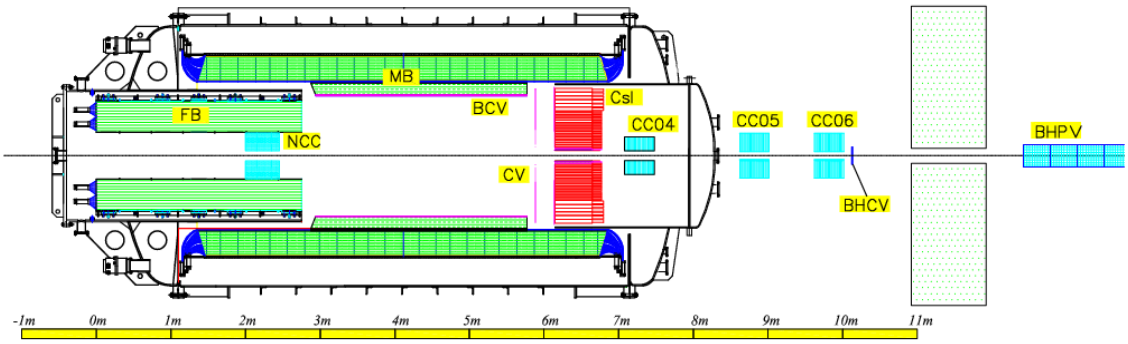

Figure 3: Schematic drawing of the detector. The components of the detector include collar counters (CCxx), Neutron Collar Counter (NCC), Front Barrel (FB), Main Barrel (MB), charged-particle vetos (BCV and CV), CsI crystals (CSI), Beam Halo Charged Veto (BHCV) and Photon Veto (BHPV).

The strategy for detecting an event is to veto any event that has charged particles or where particles do not hit the main CsI crystals, identify the two photon clusters, project back to a common decay point within the profile of the beam, select on the π^0 mass, and apply a transfer momentum cut p_T to account for the momenta of the neutrinos and reduce backgrounds.

The beam line and detector have many improvements over those from the E391a experiment. They include:

- a higher beam intensity with a factor of $\sim$40 increase id K_L flux;
- More effective halo reduction, with a reduction of the n/K_L fraction by a factor of 2-4;

- replacement of the undoped CsI crystals with those from the KTeV experiment, which have half the transverse dimensions and are 27 X_0 instead of 16 X_0 (in E391a) in length;
- replacement of collimator assemblies with new designs;
- replacement of the CV with two layers of a new design;
- redesign and replacement of the beam-hole veto detectors;
- increase the thickness of the Main Barrel photon veto; and
- develop entirely new DAQ electronics with up-to-date features.

The development of some of these items, and preparations for the experiment, will be discussed in the following sections.

4. The Neutral Beam Line

Having a well-collimated 'pencil' beam is a critical feature of the experiment's design. Multiple studies were made with both the GEANT3 [11] and FLUKA [12] Monte Carlo (MC) codes to ensure reliability.

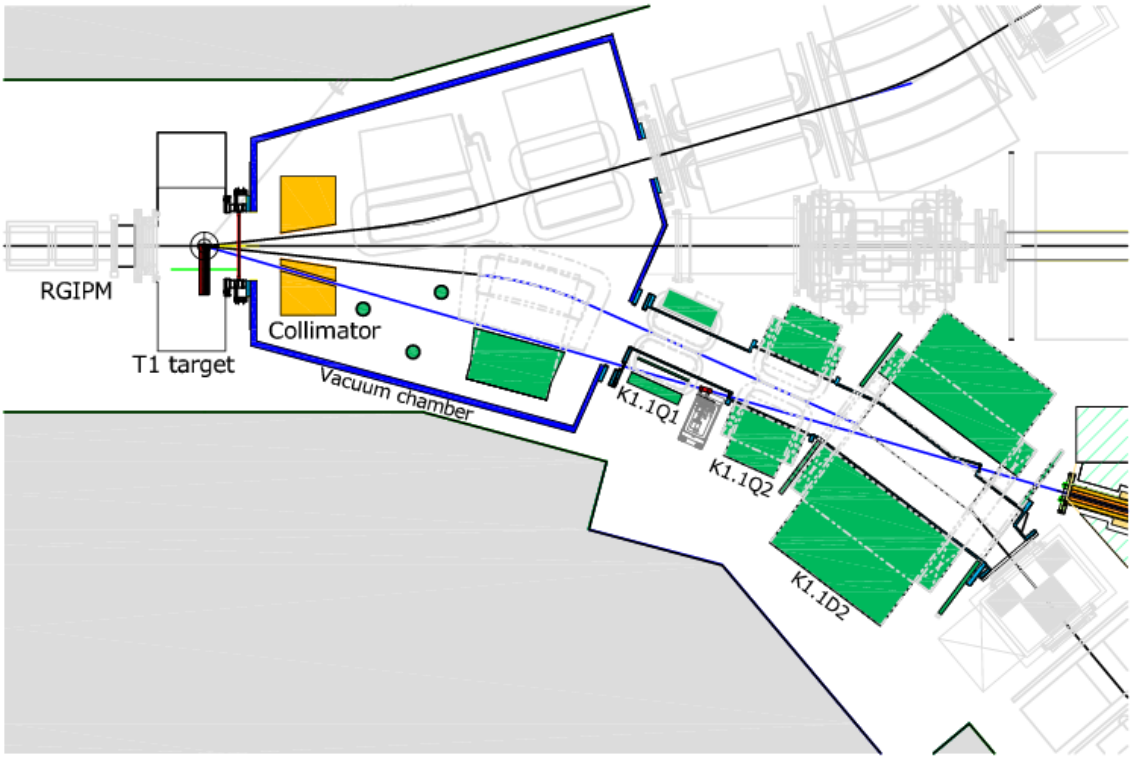

Figure 4: Layout of the upstream portion of the K_L beam line. The KOTO collimators begin near the right side.

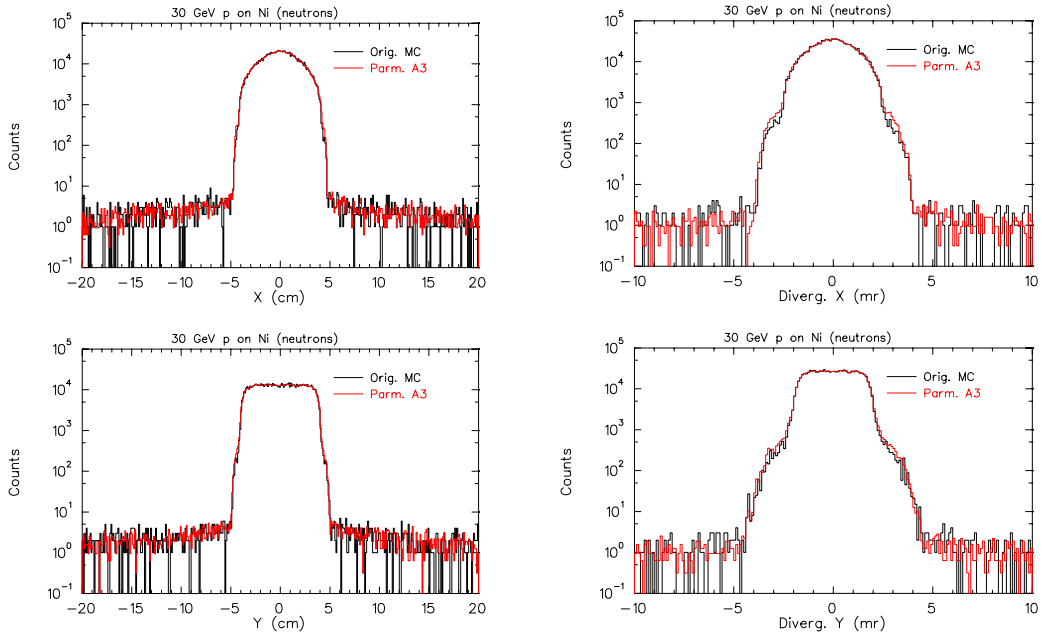

Figure 5: Left: Neutron coordinate distributions for the original MC and the parameterized results, normalized to the original MC. Right: Same for the divergences.

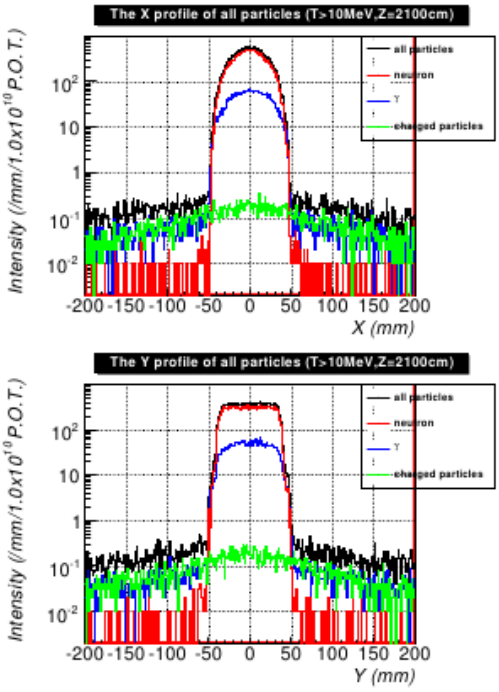

Figure 6: Beam profiles in the horizontal (upper) and vertical (lower) directions at the end of the beam line.

The upstream region of the beam line is shown in Fig. 4. It is very complicated due to the crossing of a charged-particle beam line. After being produced in air, the beam particles enter a vacuum region, pass through a small hole in a copper collimator, come very close to a magnet yoke, and continue to pass in and out of vacuum through the region. A platinum rod to absorb photons is located between the 'Q1' and 'Q2' quadrupoles. Most attention was given to the KOTO collimator region between 640 cm from the target to the end of the beam line at 2100 cm.

By tracing back the results at 2100 cm from the fluka MC, it was found that the essential kinematic features of the beam could be parameterized at 640 cm, thereby very substantially reducing computation for an unlimited number of particles. The X and Y position and divergence profiles for neutrons are compared in Fig. 5. The K_L^0 and photon profiles are very similar. The beam profiles are almost entirely contained within a square of ± 5 cm, with small divergences.

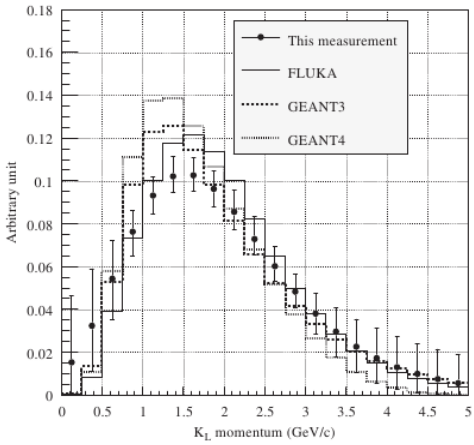

Figure 7: K_L momentum distribution at the end of the beam line. The error bars are correlated between channels. The histograms show the results of MC codes, normalized to 1 in each case.

The neutral beam profile was measured during a 2010 test run. Results are shown in Fig. 6 in comparison with MC simulations tailored to the experimental setup. The beam is very well collimated within the expected dimensions.

During the same test run, a yield equivalent to about 19×10^6 K_L^0's per spill was measured with an average momentum of about 2 GeV/c [13]. This yield is about 2.5 times the estimate in the KOTO proposal, and is higher than the E391a rate by a factor of $\sim$40.. The FLUKA code predicted a value about 10% higher, while GEANT3 and GEANT4 were lower by about 25% and a factor of 2.5, respectively [13]. The data and MC comparisons are shown in Fig. 7.

5. Data Acquisition System

A unique data acquisition system is being developed for the experiment. The requirements for the CsI calorimeter include: (1) a pipeline system with no deadtime; (2) a 14-bit full energy range and 10-bit precision for charge measurement; and (3) time resolution better than 1 ns.

An innovative feature of the system is that the signals from the CsI phototubes will be passed through specially-designed 10-pole low-pass filters and then waveform digitized into 14 bits with a 125-MHz clock. The filter converts the pulse into a fixed and stable shape that is very nearly Gaussian with a FWHM of about 45 ns. The shape can be fit to obtain precise values for both charge (energy) and time. In addition, deviations or skews are possible signs of overlapping photon clusters, or other effects. The time resolution is better than 0.5 ns for energies greater than 10 MeV; it increases to $\sim$2 ns at 1-MeV energy due to photostatistics. The scheme makes separate ADC and TDC units unnecessary. The ADC boards have been built and thoroughly tested. Additional 500-MHz boards are being built for some of the veto detectors.

The system also has trigger boards at two levels. Each ADC board will provide, for each 8-ns time step, an energy sum of all input signals through a 2.5-Gbps transceiver and fiber optics cable to a level-1 (L1) board. A full crate of L1 boards will receive the summed energies from all ADC boards, and sum them for input to a Master Control and Trigger Supervisor (MACTRIS). This unit provides the master clock for synchronization of the system, and other control functions. If the full energy sum exceeds a threshold for an event of interest, the MACTRIS will send a trigger signal to each ADC board. The signal is timed to coincide with the event of interest just before it leaves the pipeline. The data are transferred through a second 2.5-Gbps transceiver fiber optics cable to a level-2 (L2) trigger board. The L2 boards may impose additional requirements on the event, and transfer them between spills to a PC computer farm for event building and processing. The functions of the ADC and trigger boards are provided by programmed FPGA modules. The scheme is illustrated in Fig. 8.

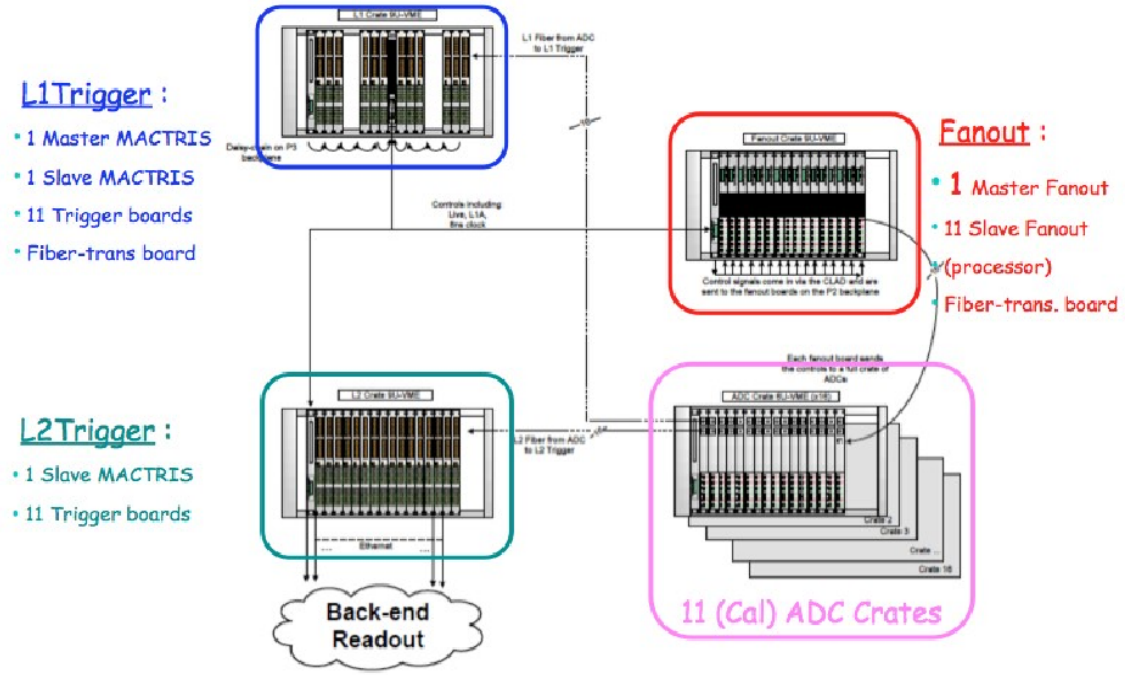

Figure 8: The DAQ electronics scheme for KOTO. There can be up to 256 ADC modules, each with 16 signal inputs.

Based on estimates from Monte Carlo simulations, including the veto detectors, the triggered event rate is estimated to be <100,000 per spill. The small fractions of halo neutrons and photons, which are dominantly at low energies, will not trigger events but might contribute to K_L^0 triggers.

If all time steps for each crystal are retained, the data that need to be stored has been estimated as up to ∼0.5 pB/day at the full design beam intensity. Of course, the data could not pass through the DAQ system without some kind of compression. Several possible schemes are being investigated, including early cluster identification and counting or bit-level compression.

One scheme that has great promise makes use of the approximately fixed, Gaussian shape of a digitized signal pulse in the ADCs. Events from early test runs have been examined and the distributions for strong peaks have been accumulated to form a standard reference peak. A correlation coefficient algorithm can then be applied for each detector signal in the ADCs. If the correlation has too small a value, all of the data for that signal can be suppressed from the L2 link. The data flow can be compressed by factors of 10–20 or more by this method. The algorithm can be applied for every signal in each 8-ns time step as the data pass through the ADC pipeline. The code has been incorporated into the ADC firmware, but has not yet been tested with beam.

6. Schedule

The J-PARC laboratory and KOTO were fortunate not to have experienced substantial damage from the major earthquake in March, 2011. There was structural damage to some buildings and roads, and the accelerator complex had to be realigned. The effects for KOTO were less, but led

to some measures to prevent future damage. The accelerator delivered beam to the Hadron Hall in January, and KOTO test runs were successfully made in February and June, 2012.

Up to the Summer 2012, the CsI crystal assembly, which includes veto detectors both inside the beam hole and outside the crystal region, have been located in a dry room. Additional detectors have been used for the tests. Beginning in July, the entire configuration is being removed, the vacuum tank from E391a will be installed, the CsI crystal assembly will be relocated inside the tank, and most of the additional veto assemblies will be installed in the tank. The work is expected to last until late in 2012, at which time an engineering run will be started. The available beam rate may be only 5-10% of the maximum design intensity, and should allow for thorough testing of all detector systems and the DAQ electronics.

The first physics run is anticipated for the Spring 2013. Based on the error range of the measured $K^+ \to \pi^+ \nu\bar{\nu}$ decay rate and the Grossman-Nir relationship, the E391a upper limit on the $K_L^0 \to \pi^0 \nu\bar{\nu}$ decay rate needs to be improved by a factor of 15-90 to get below the Grossman-Nir limit. There is high confidence that this goal can be achieved in just a few weeks of running time. *Hence, the KOTO experiment is poised to soon detect new physics Beyond the Standard Model, such as evidence for a fourth quark generation, if it exists.*

Following this initial run, there will be a shutdown in the Summer 2013 for accelerator upgrades and for completion of the full KOTO detector system. Subsequent runs will be directed to obtaining the additional factor of 10-100 needed to reach the sensitivity level of the Standard Model for the $K_L^0 \to \pi^0 \nu\bar{\nu}$ decay. Planning for the next phase of the experiment to obtain 100 or more SM events is also underway.

References

[1] N. Cabibbo, Phys. Rev. Lett. **10**, 531 (1963).

[2] S. L. Glashow, J. Iliopoulos, and L. Maiani, Phys. Rev. D **2**, 1585 (1970).

[3] J. H. Christenson *et al.*, Phys. Rev. Lett. **13**, 138 (1964).

[4] M. Kobayashi and K. Maskawa, Prog. Theor. Phys. **49**, 652 (1973).

[5] J. Brod, M. Gorbahn, and E. Stamou, Phys. Rev. D **83**, 034030 (2011).

[6] A. V. Artamonov *et al.*, Phys. Rev. D **79**, 092004 (2009), and references therein.

[7] J. K. Ahn *et al.*, Phys. Rev. **81**, 072004 (2010).

[8] Y. Grossman and Y. Nir, Phys. Letters B **398**, 163 (1997).

[9] A. J. Buras *et al.*, JHEP **1009**, 106 (2010) [arXiv:1002.2126].

[10] T. Hattori, T. Hasuike, and S. Wakaizumi, Phys. Rev. D **60**, 113008 (1999).

[11] CERN Application Software Group, GEANT Detector Description and Simulation Tool, W5013, CERN (1993).

[12] See http://www.fluka.org/fluka.php and references therein.

[13] K. Shiomi *et al.*, Nucl. Instrum. Methods Res. A **664**, 264 (2012).